

**Measurements of branching fractions for  $B^0 \rightarrow D_s^+ \pi^-$  and  $\bar{B}^0 \rightarrow D_s^+ K^-$** 

A. Das,<sup>43</sup> T. Aziz,<sup>43</sup> K. Trabelsi,<sup>9</sup> G. B. Mohanty,<sup>43</sup> I. Adachi,<sup>9</sup> H. Aihara,<sup>47</sup> K. Arinstein,<sup>1,35</sup> V. Aulchenko,<sup>1,35</sup>  
 T. Aushev,<sup>22,15</sup> A. M. Bakich,<sup>42</sup> V. Balagura,<sup>15</sup> E. Barberio,<sup>26</sup> K. Belous,<sup>13</sup> V. Bhardwaj,<sup>37</sup> B. Bhuyan,<sup>10</sup>  
 M. Bischofberger,<sup>28</sup> A. Bondar,<sup>1,35</sup> A. Bozek,<sup>32</sup> M. Bračko,<sup>24,16</sup> T. E. Browder,<sup>8</sup> Y. Chao,<sup>31</sup> A. Chen,<sup>29</sup> K.-F. Chen,<sup>31</sup>  
 P. Chen,<sup>31</sup> B. G. Cheon,<sup>7</sup> C.-C. Chiang,<sup>31</sup> I.-S. Cho,<sup>52</sup> Y. Choi,<sup>41</sup> J. Dalseno,<sup>25,44</sup> M. Danilov,<sup>15</sup> Z. Doležal,<sup>2</sup> Z. Drásal,<sup>2</sup>  
 A. Drutskoy,<sup>4</sup> W. Dungel,<sup>12</sup> S. Eidelman,<sup>1,35</sup> S. Esen,<sup>4</sup> N. Gabyshev,<sup>1,35</sup> H. Ha,<sup>20</sup> K. Hayasaka,<sup>27</sup> H. Hayashii,<sup>28</sup> Y. Horii,<sup>46</sup>  
 Y. Hoshi,<sup>45</sup> W.-S. Hou,<sup>31</sup> H. J. Hyun,<sup>21</sup> T. Iijima,<sup>27</sup> K. Inami,<sup>27</sup> R. Itoh,<sup>9</sup> M. Iwabuchi,<sup>52</sup> Y. Iwasaki,<sup>9</sup> N. J. Joshi,<sup>43</sup>  
 T. Julius,<sup>26</sup> D. H. Kah,<sup>21</sup> J. H. Kang,<sup>52</sup> P. Kapusta,<sup>32</sup> H. Kawai,<sup>3</sup> T. Kawasaki,<sup>34</sup> H. Kichimi,<sup>9</sup> C. Kiesling,<sup>25</sup> H. J. Kim,<sup>21</sup>  
 H. O. Kim,<sup>21</sup> J. H. Kim,<sup>19</sup> M. J. Kim,<sup>21</sup> Y. J. Kim,<sup>6</sup> K. Kinoshita,<sup>4</sup> B. R. Ko,<sup>20</sup> P. Kodyš,<sup>2</sup> S. Korpar,<sup>24,16</sup> P. Križan,<sup>23,16</sup>  
 P. Krokovny,<sup>9</sup> T. Kuhr,<sup>18</sup> R. Kumar,<sup>37</sup> T. Kumita,<sup>48</sup> Y.-J. Kwon,<sup>52</sup> S.-H. Kyeong,<sup>52</sup> J. S. Lange,<sup>5</sup> M. J. Lee,<sup>40</sup> S.-H. Lee,<sup>20</sup>  
 J. Li,<sup>8</sup> C. Liu,<sup>39</sup> Y. Liu,<sup>31</sup> D. Liventsev,<sup>15</sup> R. Louvot,<sup>22</sup> J. MacNaughton,<sup>9</sup> A. Matyja,<sup>32</sup> S. McOnie,<sup>42</sup> K. Miyabayashi,<sup>28</sup>  
 H. Miyata,<sup>34</sup> Y. Miyazaki,<sup>27</sup> T. Mori,<sup>27</sup> E. Nakano,<sup>36</sup> M. Nakao,<sup>9</sup> S. Neubauer,<sup>18</sup> S. Nishida,<sup>9</sup> O. Nitoh,<sup>49</sup> T. Ohshima,<sup>27</sup>  
 S. Okuno,<sup>17</sup> S. L. Olsen,<sup>40,8</sup> W. Ostrowicz,<sup>32</sup> G. Pakhlova,<sup>15</sup> C. W. Park,<sup>41</sup> H. Park,<sup>21</sup> H. K. Park,<sup>21</sup> K. S. Park,<sup>41</sup>  
 R. Pestotnik,<sup>16</sup> M. Petrič,<sup>16</sup> L. E. Piilonen,<sup>50</sup> M. Röhrken,<sup>18</sup> S. Ryu,<sup>40</sup> H. Sahoo,<sup>8</sup> K. Sakai,<sup>34</sup> Y. Sakai,<sup>9</sup> O. Schneider,<sup>22</sup>  
 K. Senyo,<sup>27</sup> M. E. Sevier,<sup>26</sup> M. Shapkin,<sup>13</sup> V. Shebalin,<sup>1,35</sup> C. P. Shen,<sup>8</sup> J.-G. Shiu,<sup>31</sup> B. Shwartz,<sup>1,35</sup> F. Simon,<sup>25,44</sup>  
 J. B. Singh,<sup>37</sup> R. Sinha,<sup>14</sup> P. Smerkol,<sup>16</sup> A. Sokolov,<sup>13</sup> E. Solovieva,<sup>15</sup> M. Starič,<sup>16</sup> T. Sumiyoshi,<sup>48</sup> S. Suzuki,<sup>38</sup>  
 Y. Teramoto,<sup>36</sup> S. Uehara,<sup>9</sup> T. Uglov,<sup>15</sup> Y. Unno,<sup>7</sup> S. Uno,<sup>9</sup> Y. Usov,<sup>1,35</sup> G. Varner,<sup>8</sup> K. Vervink,<sup>22</sup> C. H. Wang,<sup>30</sup> P. Wang,<sup>11</sup>  
 M. Watanabe,<sup>34</sup> Y. Watanabe,<sup>17</sup> K. M. Williams,<sup>50</sup> E. Won,<sup>20</sup> Y. Yamashita,<sup>33</sup> M. Yamauchi,<sup>9</sup> C. C. Zhang,<sup>11</sup> Z. P. Zhang,<sup>39</sup>  
 V. Zhilich,<sup>1,35</sup> P. Zhou,<sup>51</sup> V. Zhulanov,<sup>1,35</sup> A. Zupanc,<sup>18</sup> and O. Zyukova<sup>1,35</sup>

(The Belle Collaboration)

<sup>1</sup>*Budker Institute of Nuclear Physics, Novosibirsk*<sup>2</sup>*Faculty of Mathematics and Physics, Charles University, Prague*<sup>3</sup>*Chiba University, Chiba*<sup>4</sup>*University of Cincinnati, Cincinnati, Ohio 45221*<sup>5</sup>*Justus-Liebig-Universität Gießen, Gießen*<sup>6</sup>*The Graduate University for Advanced Studies, Hayama*<sup>7</sup>*Hanyang University, Seoul*<sup>8</sup>*University of Hawaii, Honolulu, Hawaii 96822*<sup>9</sup>*High Energy Accelerator Research Organization (KEK), Tsukuba*<sup>10</sup>*Indian Institute of Technology Guwahati, Guwahati*<sup>11</sup>*Institute of High Energy Physics, Chinese Academy of Sciences, Beijing*<sup>12</sup>*Institute of High Energy Physics, Vienna*<sup>13</sup>*Institute of High Energy Physics, Protvino*<sup>14</sup>*Institute of Mathematical Sciences, Chennai*<sup>15</sup>*Institute for Theoretical and Experimental Physics, Moscow*<sup>16</sup>*J. Stefan Institute, Ljubljana*<sup>17</sup>*Kanagawa University, Yokohama*<sup>18</sup>*Institut für Experimentelle Kernphysik, Karlsruher Institut für Technologie, Karlsruhe*<sup>19</sup>*Korea Institute of Science and Technology Information, Daejeon*<sup>20</sup>*Korea University, Seoul*<sup>21</sup>*Kyungpook National University, Taegu*<sup>22</sup>*École Polytechnique Fédérale de Lausanne (EPFL), Lausanne*<sup>23</sup>*Faculty of Mathematics and Physics, University of Ljubljana, Ljubljana*<sup>24</sup>*University of Maribor, Maribor*<sup>25</sup>*Max-Planck-Institut für Physik, München*<sup>26</sup>*University of Melbourne, School of Physics, Victoria 3010*<sup>27</sup>*Nagoya University, Nagoya*<sup>28</sup>*Nara Women's University, Nara*<sup>29</sup>*National Central University, Chung-li*<sup>30</sup>*National United University, Miao Li*<sup>31</sup>*Department of Physics, National Taiwan University, Taipei*<sup>32</sup>*H. Niewodniczanski Institute of Nuclear Physics, Krakow*<sup>33</sup>*Nippon Dental University, Niigata*

- <sup>34</sup>*Niigata University, Niigata*  
<sup>35</sup>*Novosibirsk State University, Novosibirsk*  
<sup>36</sup>*Osaka City University, Osaka*  
<sup>37</sup>*Panjab University, Chandigarh*  
<sup>38</sup>*Saga University, Saga*  
<sup>39</sup>*University of Science and Technology of China, Hefei*  
<sup>40</sup>*Seoul National University, Seoul*  
<sup>41</sup>*Sungkyunkwan University, Suwon*  
<sup>42</sup>*School of Physics, University of Sydney, NSW 2006*  
<sup>43</sup>*Tata Institute of Fundamental Research, Mumbai*  
<sup>44</sup>*Excellence Cluster Universe, Technische Universität München, Garching*  
<sup>45</sup>*Tohoku Gakuin University, Tagajo*  
<sup>46</sup>*Tohoku University, Sendai*  
<sup>47</sup>*Department of Physics, University of Tokyo, Tokyo*  
<sup>48</sup>*Tokyo Metropolitan University, Tokyo*  
<sup>49</sup>*Tokyo University of Agriculture and Technology, Tokyo*  
<sup>50</sup>*IPNAS, Virginia Polytechnic Institute and State University, Blacksburg, Virginia 24061*  
<sup>51</sup>*Wayne State University, Detroit, Michigan 48202*  
<sup>52</sup>*Yonsei University, Seoul*

(Received 28 July 2010; published 28 September 2010)

We present improved measurements of the branching fractions for the decays  $B^0 \rightarrow D_s^+ \pi^-$  and  $\bar{B}^0 \rightarrow D_s^+ K^-$  using a data sample of  $657 \times 10^6 B\bar{B}$  events collected at the  $\Upsilon(4S)$  resonance with the Belle detector at the KEKB asymmetric-energy  $e^+e^-$  collider. The results are  $\mathcal{B}(B^0 \rightarrow D_s^+ \pi^-) = (1.99 \pm 0.26 \pm 0.18) \times 10^{-5}$  and  $\mathcal{B}(\bar{B}^0 \rightarrow D_s^+ K^-) = (1.91 \pm 0.24 \pm 0.17) \times 10^{-5}$ , where the uncertainties are statistical and systematic, respectively. Based on these results, we determine the ratio between amplitudes of the doubly Cabibbo suppressed decay  $B^0 \rightarrow D^+ \pi^-$  and the Cabibbo favored decay  $B^0 \rightarrow D^- \pi^+$ ,  $R_{D\pi} = [1.71 \pm 0.11(\text{stat}) \pm 0.09(\text{syst}) \pm 0.02(\text{theo})]\%$ , where the last term denotes the theory error.

DOI: 10.1103/PhysRevD.82.051103

PACS numbers: 13.25.Hw, 12.15.Hh, 11.30.Er

In the standard model (SM),  $CP$  violation occurs due to a single irreducible phase appearing in the quark-flavor mixing matrix, called the Cabibbo-Kobayashi-Maskawa (CKM) matrix [1], which relates the weak interaction eigenstates to those of mass. Unitarity of the CKM matrix yields relationships between its elements that can be depicted as triangles in the complex plane [2].  $B$  meson decays offer a variety of ways to measure the angles and sides of the unitarity triangle (UT), formed from elements in the first and third columns of the CKM matrix, and hence to verify the  $CP$  violation mechanism of the SM.

Of particular interest is the decay  $B^0 \rightarrow D_s^+ \pi^-$ , which is dominated by the tree level  $b \rightarrow u$  transition shown in Fig. 1(a). Assuming SU(3) flavor symmetry, one can use this decay channel to determine the ratio between amplitudes of the doubly Cabibbo suppressed decay  $B^0 \rightarrow D^+ \pi^-$  and the Cabibbo favored decay  $B^0 \rightarrow D^- \pi^+$  [3]

$$R_{D\pi} = \tan\theta_C \frac{f_D}{f_{D_s}} \sqrt{\frac{\mathcal{B}(B^0 \rightarrow D_s^+ \pi^-)}{\mathcal{B}(B^0 \rightarrow D^- \pi^+)}} \quad (1)$$

where  $\theta_C$  is the Cabibbo angle,  $f_D(f_{D_s})$  is the  $D(D_s)$  meson decay constant, and  $\mathcal{B}(B^0 \rightarrow D_s^+ \pi^-)$  and  $\mathcal{B}(B^0 \rightarrow D^- \pi^+)$  are the branching fractions of  $B^0 \rightarrow D_s^+ \pi^-$  and  $B^0 \rightarrow D^- \pi^+$ . In Figs. 1(b) and 1(c) we show the dominant Feynman diagrams for the decays  $B^0 \rightarrow D^\mp \pi^\pm$ . The ratio  $R_{D\pi}$  is an important input for the determination of the UT

angle  $\phi_3$ , since the measurement of time-dependent  $CP$  violation in  $B^0 \rightarrow D^\mp \pi^\pm$  [4] determines only the quantity  $R_{D\pi} \sin(2\phi_1 + \phi_3)/(1 + R_{D\pi}^2)$ , where  $\phi_1$  is the most precisely measured angle of the UT [5,6]. Furthermore, it has also been suggested [7] that the CKM matrix element  $|V_{ub}|$  (related to one of the sides of the UT) can be extracted from the measured branching fraction of  $B^0 \rightarrow D_s^+ \pi^-$ .

The decay  $\bar{B}^0 \rightarrow D_s^+ K^-$  occurs via the internal  $W$ -exchange diagram [see Fig. 1(d)]. Potential contributions arising from rescattering effects [8] could enhance its branching fraction. Recent studies [9], however, find the rescattering contribution to be negligible. Furthermore, the calculation of  $R_{D\pi}$  in Ref. [3] assumes that the size of the  $W$ -exchange amplitude in  $B^0 \rightarrow D^\mp \pi^\pm$  [Figs. 1(e) and 1(f)] is small compared to the corresponding tree amplitude. One can verify this hypothesis with an accurate measurement of  $\mathcal{B}(\bar{B}^0 \rightarrow D_s^+ K^-)$ . In the absence of rescattering the exchange diagram is the sole contributor to  $\bar{B}^0 \rightarrow D_s^+ K^-$ , and hence it provides a measure of the  $W$ -exchange contribution in  $B^0 \rightarrow D^\mp \pi^\pm$ .

The decay channels  $B^0 \rightarrow D_s^+ \pi^-$  and  $\bar{B}^0 \rightarrow D_s^+ K^-$  have been previously studied by the Belle [10] and BABAR [11] collaborations. In this paper, we present improved measurements of the branching fractions  $\mathcal{B}(B^0 \rightarrow D_s^+ \pi^-)$  and  $\mathcal{B}(\bar{B}^0 \rightarrow D_s^+ K^-)$  based on a data sample of  $657 \times 10^6 B\bar{B}$  decays, which is close to 8 times the size of the one used in our earlier result [10]. The data were

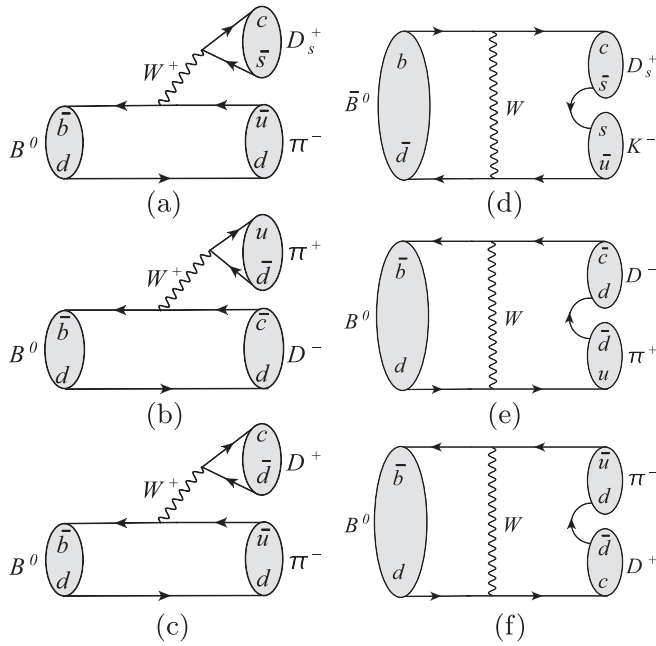


FIG. 1. Feynman diagrams for (a)  $B^0 \rightarrow D_s^+ \pi^-$ ; (b) the Cabibbo favored decay  $B^0 \rightarrow D^- \pi^+$ ; (c) the doubly Cabibbo suppressed decay  $B^0 \rightarrow D^+ \pi^-$ ; and the color suppressed  $W$ -exchange contribution to (d)  $\bar{B}^0 \rightarrow D_s^+ K^-$ , (e)  $B^0 \rightarrow D^- \pi^+$ , and (f)  $B^0 \rightarrow D^+ \pi^-$ .

collected with the Belle detector at the KEKB asymmetric-energy  $e^+e^-$  collider [12]. A detailed description of the Belle detector can be found elsewhere [13].

We select  $B^0 \rightarrow D_s^+ \pi^-$  and  $\bar{B}^0 \rightarrow D_s^+ K^-$  decay candidates [14] from events that have four or more charged tracks. Each track is required to be well measured in a tracking system that consists of a silicon vertex detector and a central drift chamber (both operating in a 1.5 T magnetic field), and to originate from the interaction point (IP). Track candidates must have a minimum transverse momentum of 100 MeV/c, and a distance of closest approach with respect to the IP less than 0.2 cm in the  $r$ - $\phi$  plane, which is perpendicular to the  $z$  axis, and less than 4.0 cm along the  $z$  axis, where the  $z$  axis is defined by the direction opposite to the  $e^+$  beam. Charged pions and kaons are identified by combining particle identification (PID) information obtained with various subdetectors: ionization energy loss from the drift chamber, time-of-flight information from an array of scintillation counters, and the number of photoelectrons from an aerogel Cherenkov counter system. We distinguish kaons from pions using a likelihood ratio,  $\mathcal{R}_{K/\pi} = \mathcal{L}_K / (\mathcal{L}_K + \mathcal{L}_\pi)$ , where  $\mathcal{L}_K$  ( $\mathcal{L}_\pi$ ) is the likelihood value for the kaon (pion) hypothesis. We require  $\mathcal{R}_{K/\pi}$  to be greater than 0.6 for kaon candidates, while tracks failing this requirement are classified as pions. The efficiency for kaon (pion) identification ranges between 84% to 98% (92% to 94%) depending on the track momentum with a pion (kaon) fake rate of about 8% (16%).

We reconstruct  $D_s^+$  mesons in three decay modes:  $D_s^+ \rightarrow \phi \pi^+$ ,  $\bar{K}^{*0} K^+$ , and  $K_S^0 K^+$ . The  $\phi$  ( $\bar{K}^{*0}$ ) mesons are formed from  $K^+ K^-$  ( $K^- \pi^+$ ) pairs having invariant masses that lie within 14 MeV/ $c^2$  (75 MeV/ $c^2$ ) of the nominal  $\phi$  ( $\bar{K}^{*0}$ ) mass [15]. Note that for kaons originating from a  $\phi$  decay we relax the  $\mathcal{R}_{K/\pi}$  requirement to 0.1 due to the small background contribution. To reduce combinatorial background, we require  $|\cos\theta_H| > 0.3$  for the  $D_s^+ \rightarrow \phi \pi^+$  ( $D_s^+ \rightarrow \bar{K}^{*0} K^+$ ) mode, where  $\theta_H$  is the angle between decay products of the  $\phi$  ( $\bar{K}^{*0}$ ) and the flight direction of the  $D_s^+$  meson in the rest frame of the  $\phi$  ( $\bar{K}^{*0}$ ). We reconstruct  $K_S^0$  mesons through the channel  $K_S^0 \rightarrow \pi^+ \pi^-$ , where we require the invariant mass of two oppositely charged tracks (with the pion mass hypothesis assumed) to be within 10 MeV/ $c^2$  of the nominal  $K_S^0$  mass [15]. The  $K_S^0$  candidates must also satisfy momentum-dependent selection criteria based on their vertex topology and flight length in the  $r$ - $\phi$  plane [16]. We select  $D_s^+$  mesons in a wide mass window ( $1.92 \text{ GeV}/c^2 < M_{D_s^+} < 2.02 \text{ GeV}/c^2$ ), common to the three decay modes, for further studies. Finally we combine each  $D_s^+$  candidate with an oppositely charged pion or kaon to form a neutral  $B$  meson.

For the reconstruction of  $B$  candidates we utilize two kinematic variables: the center-of-mass (CM) energy difference,  $\Delta E = E_B - E_{\text{beam}}$ , and the beam-constrained mass,  $M_{\text{bc}} = \sqrt{E_{\text{beam}}^2 - \vec{p}_B^2}$ , where  $E_{\text{beam}}$  is the beam energy,  $E_B$  and  $\vec{p}_B$  are the energy and momentum of the  $B$  candidate measured in the CM frame, respectively ( $c = 1$  is assumed). The  $M_{\text{bc}}$  distribution for signal events peaks near the  $B$  mass, while the  $\Delta E$  distribution peaks at zero. We retain  $B$  candidates with  $5.27 \text{ GeV}/c^2 < M_{\text{bc}} < 5.30 \text{ GeV}/c^2$  and  $-0.1 \text{ GeV} < \Delta E < 0.2 \text{ GeV}$ . An asymmetric  $\Delta E$  requirement is imposed to suppress background contributions from  $B$  decays, such as  $B^0 \rightarrow D_s^{*+} \pi^-$  and  $\bar{B}^0 \rightarrow D_s^{*+} K^-$ , at negative  $\Delta E$  values.

About 5% of the selected  $B^0 \rightarrow D_s^+ \pi^-$  and  $\bar{B}^0 \rightarrow D_s^+ K^-$  events contain multiple  $B$  candidates. In such cases we choose the one with the  $M_{\text{bc}}$  value closest to the nominal  $B^0$  mass [15]. In order to determine the background reduction criteria (described below), signal and background yields are estimated in the signal region with the requirements that  $|\Delta E| < 30 \text{ MeV}$  and that  $M_{D_s^+}$  be within 13 MeV/ $c^2$ , 15 MeV/ $c^2$ , and 17 MeV/ $c^2$  of the nominal  $D_s^+$  mass for  $\phi \pi^+$ ,  $\bar{K}^{*0} K^+$ , and  $K_S^0 K^+$ , respectively. These requirements roughly correspond to a  $\pm 3\sigma$  window in resolution.

Continuum  $e^+e^- \rightarrow q\bar{q}$  ( $q = u, d, s$ , and  $c$  quarks) events are the dominant background. To discriminate the jetlike continuum background from signal we use modified Fox-Wolfram moments [17] that are combined into a Fisher discriminant. We further combine the Fisher output with the cosine of the angle between the  $B$  flight direction in the CM frame and the  $z$  axis, to form a likelihood ratio  $\mathcal{R} = \mathcal{L}_{\text{sig}} / (\mathcal{L}_{\text{sig}} + \mathcal{L}_{q\bar{q}})$ . Here,  $\mathcal{L}_{\text{sig}}$  and  $\mathcal{L}_{q\bar{q}}$  are the

likelihood functions for signal and continuum events obtained with Monte Carlo (MC) simulations [18]. We impose separate requirements on  $\mathcal{R}$  for the three decay modes in both  $B^0 \rightarrow D_s^+ \pi^-$  and  $\bar{B}^0 \rightarrow D_s^+ K^-$ . These requirements are obtained by maximizing a figure of merit,  $S/\sqrt{S+B}$ , where  $S$  and  $B$  are the number of signal and  $q\bar{q}$  events expected in the signal region, calculated using MC simulated events. The requirements on  $\mathcal{R}$  remove 92% (78%) of continuum background while retaining 75% (86%) of signal events for  $B^0 \rightarrow D_s^+ \pi^-$  ( $\bar{B}^0 \rightarrow D_s^+ K^-$ ).

A large MC sample of  $B\bar{B}$  events is used to determine possible backgrounds that can contaminate our signal region. The decay  $\bar{B}^0 \rightarrow D^+ \pi^-$ ,  $D^+ \rightarrow K^- \pi^+ \pi^+$  including  $D^+ \rightarrow \bar{K}^{*0} \pi^+$  and  $K_0^{*0}(1430) \pi^+$ , where a pion is misidentified as a kaon, poses a particular challenge for the  $B^0 \rightarrow D_s^+ \pi^-$  channel. This decay mode has a large branching fraction; its reconstructed invariant-mass spectrum peaks near the  $D_s^+$  peak while its  $\Delta E$  distribution is shifted by about 70 MeV from zero. The  $\bar{B}^0 \rightarrow D^+ \pi^-$  background is more prominent in  $D_s^+ \rightarrow \bar{K}^{*0} K^+$  compared to  $D_s^+ \rightarrow \phi \pi^+$  because of the wider invariant-mass requirement. To suppress this background, we reject event candidates that are consistent with the  $D^+ \rightarrow K^- \pi^+ \pi^+$  mass hypothesis within 16 MeV/ $c^2$  ( $\sim 3\sigma$ ) when the two same-sign particles in the  $D_s^+$  candidate are assigned to be pions. For the  $D_s^+ \rightarrow K_S^0 K^+$  mode there is a similar background from  $\bar{B}^0 \rightarrow D^+ \pi^-$ ,  $D^+ \rightarrow K_S^0 \pi^+$ . Here we exclude candidates consistent within 20 MeV/ $c^2$  with the  $D^+ \rightarrow K_S^0 \pi^+$  mass hypothesis. The channel  $\bar{B}^0 \rightarrow D_s^+ K^-$  has a similar reflection background from  $\bar{B}^0 \rightarrow D^+ K^-$ ,  $D^+ \rightarrow K^- \pi^+ \pi^+$ . We apply the same rejection criteria, as in  $B^0 \rightarrow D_s^+ \pi^-$ , to the invariant mass of the  $K^- \pi^+ \pi^+$  system. Our invariant-mass veto requirements also reduce a similar background from  $\bar{B}^0 \rightarrow D^{*+} \pi^-$ ,  $D^{*+} \rightarrow D^+ \pi^0$ .

Another  $B\bar{B}$  background arises from charmless decays such as  $B^0 \rightarrow K_S^0 K^- \pi^+$ ,  $K_S^0 K^+ K^-$ ,  $\bar{K}^{*0} K^+ K^-$ , and  $\phi K^- \pi^+$ . These events peak at  $\Delta E = 0$  as the final state is the same as signal, but have a broad nonpeaking  $D_s^+$  mass distribution due to the absence of a  $D_s^+$  in the final state. Finally, there is a crossfeed contribution from  $\bar{B}^0 \rightarrow D_s^+ K^-$  ( $B^0 \rightarrow D_s^+ \pi^-$ ) to  $B^0 \rightarrow D_s^+ \pi^-$  ( $\bar{B}^0 \rightarrow D_s^+ K^-$ ) due to a kaon (pion) faking a pion (kaon), which also needs to be considered.

To determine the branching fractions of  $B^0 \rightarrow D_s^+ \pi^-$  and  $\bar{B}^0 \rightarrow D_s^+ K^-$ , we perform an unbinned extended maximum likelihood fit to the candidate events found in the selected regions of  $M_{bc}$ ,  $\Delta E$ , and  $M_{D_s^+}$  (described above). The probability density functions (PDFs) are functions of  $\Delta E$  and  $M_{D_s^+}$ . The extended likelihood function is

$$\mathcal{L} = \frac{e^{-\left(\sum_{j,m} Y_{jm}\right)}}{N!} \prod_{i=1}^N \left\{ \sum_j Y_{jm} \mathcal{P}_{jm}(\vec{x}_i) \right\}, \quad (2)$$

where  $Y_{jm}$  is the yield of event category  $j$  for  $D_s^+$  decay mode  $m$  ( $\phi \pi^+$ ,  $\bar{K}^{*0} K^+$ , or  $K_S^0 K^+$ ),  $N$  is the total number of

candidate events in three  $D_s^+$  modes, and  $\mathcal{P}_{jm}(\vec{x}_i)$  is the PDF evaluated for the variables  $\vec{x} \equiv (\Delta E, M_{D_s^+})$  measured for event  $i$ . To constrain the three  $D_s^+$  modes to have a common branching fraction, we express the signal ( $j = 1$ ) yield as

$$Y_{1m} = N_{B\bar{B}} \mathcal{B} \mathcal{B}_m \epsilon_m, \quad (3)$$

where  $N_{B\bar{B}}$  is the number of  $B\bar{B}$  events,  $\mathcal{B}$  is the branching fraction of  $B^0 \rightarrow D_s^+ \pi^-$  (or,  $\bar{B}^0 \rightarrow D_s^+ K^-$ ),  $\mathcal{B}_m$  is the branching fraction of the  $D_s^+$  decay mode  $m$  [15], and  $\epsilon_m$  is the detection efficiency of the corresponding decay mode. Finally to account for crossfeeds between the two signal channels, they are simultaneously fitted, with the  $\bar{B}^0 \rightarrow D_s^+ K^-$  signal yield in the correctly reconstructed sample determining the normalization of the crossfeed in the  $B^0 \rightarrow D_s^+ \pi^-$  fit region, and vice versa.

There are four PDF components, each denoting an event category, for the  $D_s^+$  decay modes considered: signal, crossfeed, combinatorial, and charmless backgrounds. The signal  $\Delta E$  PDF shape is modeled with the sum of two Gaussian functions with a common ratio of the narrow component to the total for the three  $D_s^+$  modes. We parametrize the signal  $M_{D_s^+}$  distribution using the sum of two Gaussians with a common mean and ratio of areas for all the  $D_s^+$  modes, and use the same PDF for both the  $D_s^+ \pi^-$  and  $D_s^+ K^-$  channels. We use an asymmetric Gaussian to model the  $\Delta E$  distribution of the  $D_s^+ \pi^-$  ( $D_s^+ K^-$ ) crossfeed, that contributes to the  $\bar{B}^0 \rightarrow D_s^+ K^-$  ( $B^0 \rightarrow D_s^+ \pi^-$ ) signal. Combinatorial background arises when a random track is combined with a correctly reconstructed or misreconstructed  $D_s^+$  candidate. This background is mostly from generic  $B\bar{B}$  and continuum  $q\bar{q}$  processes. To model misreconstructed  $D_s^+$  candidates we use a linear function to describe the  $M_{D_s^+}$  distribution, while the signal  $M_{D_s^+}$  PDF shape is used for the combinatorial background that contains correctly reconstructed  $D_s^+$  candidates. The  $\Delta E$  distribution in both cases is parametrized with a linear function. Charmless background events are characterized by a linear  $M_{D_s^+}$  distribution and a peaking  $\Delta E$ , which is modeled with the signal PDF shape. For both signal and background PDF parametrizations, we obtain shape parameters from the corresponding MC samples.

We calibrate various PDF shape parameters obtained from MC events using a large-statistics control sample of  $\bar{B}^0 \rightarrow D^+ \pi^-$ ;  $D^+ \rightarrow \phi \pi^+$ ,  $\bar{K}^{*0} K^+$ , and  $K_S^0 K^+$ . The peak positions and widths are adjusted based on the difference between data and MC simulations observed in the control channel. We find the measured branching fraction of the control sample is in agreement with the current world-average value. We also cross-check our analysis procedure by applying it to a data sample enriched with the Cabibbo suppressed decay  $\bar{B}^0 \rightarrow D^+ K^-$ , where the  $D^+$  decays to  $\phi \pi^+$ ,  $\bar{K}^{*0} K^+$ , and  $K_S^0 K^+$ . The measured branching fraction is found to be consistent with the world-average value.

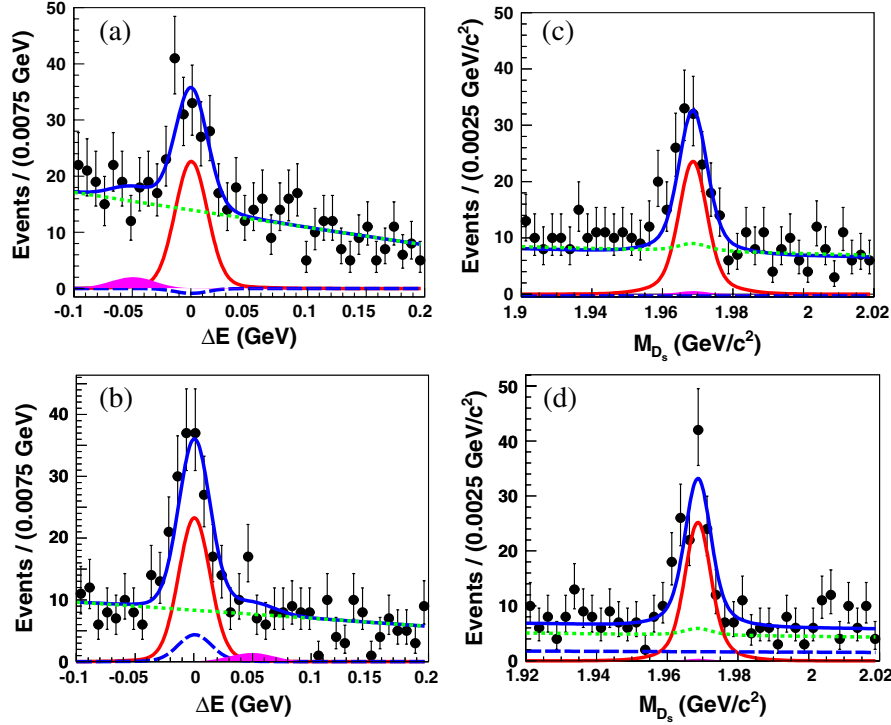


FIG. 2 (color online). Projections of the simultaneous fit to (a, c)  $B^0 \rightarrow D_s^+ \pi^-$  and (b, d)  $B^0 \rightarrow D_s^+ K^-$ . (a, b) correspond to  $\Delta E$  and (c, d) are the  $D_s^+$  mass distributions. Points with error bars show the data, the blue solid curves are the total fit result, the red solid curves are the signal component, the magenta filled curves represent the crossfeed contribution, the green dotted curves are the combinatorial background, and the blue dashed curves correspond to the charmless  $B$  background.

Our fit in total has 32 free parameters. They are the branching fractions of both the decay channels (2); the yields of the charmless background (6), the combinatorial background with correctly reconstructed  $D_s^+$  candidates (6), and the pure combinatorial background (6); and the slopes of the linear functions representing the nonpeaking  $\Delta E$  shape (6), and the nonpeaking  $M_{D_s^+}$  shape (6). Figure 2 shows results of the simultaneous fit for both the signal channels, projected onto  $\Delta E$  and  $M_{D_s^+}$ . For  $\Delta E$  ( $M_{D_s^+}$ ) projections we apply the  $M_{D_s^+}$  ( $\Delta E$ ) signal region requirement, as described earlier. In Table I we summarize the fit results. The signal significance is calculated as

$\sqrt{-2 \ln(\mathcal{L}_0 / \mathcal{L}_{\max})}$ , where  $\mathcal{L}_{\max}$  is the maximum likelihood value for the nominal data fit, and  $\mathcal{L}_0$  is the corresponding value with the signal yield fixed to zero. Including systematic errors (described below), which impact only the signal yield, into the statistical likelihood curve, through a Gaussian convolution, we determine the significance to be 8.0 and 9.2 standard deviations for  $B^0 \rightarrow D_s^+ \pi^-$  and  $B^0 \rightarrow D_s^+ K^-$ , respectively.

Systematic uncertainties that affect our measurement are summarized in Table II. The dominant one is the error on the current world-average values of the  $D_s^+$  decay branching fractions [15]. The remaining sources of systematic error

TABLE I. Efficiency ( $\epsilon$ ), signal yield ( $N_{\text{sig}}$ ), charmless background yield ( $N_{\text{chmls}}$ ), and branching fraction ( $\mathcal{B}$ ) from fits to the data obtained individually in the three  $D_s^+$  modes as well as from the simultaneous fit. Individual branching fraction results (statistical errors only) are consistent with each other and with that from the simultaneous fit, where the systematic error and signal significance ( $\mathcal{S}$ ) are also quoted.

$B$ mode	$D_s^+$ mode	$\epsilon$ (%)	$N_{\text{sig}}$	$N_{\text{chmls}}$	$\mathcal{B}(10^{-5})$	$\mathcal{S}(\sigma)$
$B^0 \rightarrow D_s^+ \pi^-$	$\phi(K^+ K^-) \pi^+$	21.6	$64 \pm 10$	$0 \pm 8$	$2.08 \pm 0.34$	
	$\bar{K}^{*0}(K^- \pi^+) K^+$	11.2	$33 \pm 9$	$-7 \pm 17$	$1.71 \pm 0.49$	
	$K_S^0 K^+$	15.7	$24 \pm 9$	$-4 \pm 13$	$2.21 \pm 0.83$	
	Simultaneous fit result				$1.99 \pm 0.26 \pm 0.18$	8.0
$B^0 \rightarrow D_s^+ K^-$	$\phi(K^+ K^-) \pi^+$	22.0	$61 \pm 10$	$14 \pm 10$	$1.97 \pm 0.31$	
	$\bar{K}^{*0}(K^- \pi^+) K^+$	11.1	$39 \pm 9$	$27 \pm 14$	$2.04 \pm 0.47$	
	$K_S^0 K^+$	14.9	$19 \pm 11$	$31 \pm 12$	$1.20 \pm 0.68$	
	Simultaneous fit result				$1.91 \pm 0.24 \pm 0.17$	9.2

TABLE II. Summary of the systematic uncertainty.

Source	Systematic contribution (%) to	
	$\mathcal{B}(B^0 \rightarrow D_s^+ \pi^-)$	$\mathcal{B}(\bar{B}^0 \rightarrow D_s^+ K^-)$
$D_s^+$ branching fraction	+6.59, -6.51	+6.31, -6.14
PDF shape	+1.44, -1.79	+1.28, -1.33
MC statistics	+0.39, -0.48	+0.46, -0.45
$K_S^0$ reconstruction	+0.45, -0.40	$\pm 0.63$
PID efficiency	$\pm 2.78$	$\pm 3.06$
Tracking efficiency	$\pm 4.00$	$\pm 4.00$
$N_{B\bar{B}}$	$\pm 1.40$	$\pm 1.40$
Requirements on $\mathcal{R}$	$\pm 1.60$	$\pm 1.60$
Fit bias	$\pm 3.42$	$\pm 2.09$
Total	+9.26, -9.27	+8.74, -8.62

are the fixed PDF shapes, for which we vary the correction factors (applied to the peak positions and widths) in accordance with their errors obtained from the control sample  $\bar{B}^0 \rightarrow D^+ \pi^-$ ; MC statistics; the efficiencies of tracking, PID, and  $K_S^0$  reconstruction; the error on  $N_{B\bar{B}}$ , assuming equal production of  $B^0 \bar{B}^0$  and  $B^+ B^-$  pairs at the  $\Upsilon(4S)$ ; requirements on  $\mathcal{R}$ , evaluated using the control sample; and the fit bias. We estimate the systematic error due to fit bias as a linear sum of the bias itself and the statistical error on it, using ensembles of simulated experiments.

We obtain the branching fractions  $\mathcal{B}(B^0 \rightarrow D_s^+ \pi^-) = (1.99 \pm 0.26 \pm 0.18) \times 10^{-5}$  and  $\mathcal{B}(\bar{B}^0 \rightarrow D_s^+ K^-) = (1.91 \pm 0.24 \pm 0.17) \times 10^{-5}$ , where the uncertainties are statistical and systematic, respectively. These results are consistent with, and constitute a significant improvement over, our previous results [10]. Using our measurement of  $B^0 \rightarrow D_s^+ \pi^-$  in conjunction with the value of Cabibbo angle [15],  $\tan\theta_C = 0.2314 \pm 0.0021$ , the lattice QCD calculation of  $f_{D_s}/f_D = 1.164 \pm 0.011$  [19], and the branching fraction  $\mathcal{B}(B^0 \rightarrow D^- \pi^+) = (2.68 \pm 0.13) \times 10^{-3}$  [15], we obtain  $R_{D\pi} = [1.71 \pm 0.11(\text{stat}) \pm 0.09(\text{syst}) \pm 0.02(\text{theo})]\%$ , where the last term accounts for the theory uncertainty in the  $f_D/f_{D_s}$  estimation. Uncertainties due to other possible SU(3) breaking effects [20], which are of order (10–15)%, are not included in the quoted theory error. This constitutes the most precise measurement of  $R_{D\pi}$  to date. The measured value of  $\mathcal{B}(\bar{B}^0 \rightarrow D_s^+ K^-)$  can be understood in terms of a pure

$W$ -exchange contribution, which is in agreement with our recent measurement of  $\bar{B}^0 \rightarrow D_s^{*+} K^-$  [21].

To conclude, using a data sample of  $657 \times 10^6 B\bar{B}$  pairs collected by Belle, we report the most precise measurement of branching fractions for the  $B^0 \rightarrow D_s^+ \pi^-$  and  $\bar{B}^0 \rightarrow D_s^+ K^-$  decays. This improves the precision of the parameter  $R_{D\pi}$ , and thus will also improve determinations of the UT angle  $\phi_3$  from  $CP$  violation measurements in  $B^0 \rightarrow D^\mp \pi^\pm$  decays. One can use the  $B^0 \rightarrow D_s^+ \pi^-$  result to calculate the CKM matrix element  $|V_{ub}|$  following the prescription laid out in Ref. [7]. Our results supersede the previous Belle measurement [10].

We thank the KEKB group for the excellent operation of the accelerator, the KEK cryogenics group for the efficient operation of the solenoid, and the KEK computer group and the National Institute of Informatics for valuable computing and SINET3 network support. We acknowledge support from the Ministry of Education, Culture, Sports, Science, and Technology (MEXT) of Japan, the Japan Society for the Promotion of Science (JSPS), and the Tau-Lepton Physics Research Center of Nagoya University; the Australian Research Council and the Australian Department of Industry, Innovation, Science and Research; the National Natural Science Foundation of China under Contract No. 10575109, 10775142, 10875115 and 10825524; the Ministry of Education, Youth and Sports of the Czech Republic under Contract No. LA10033 and MSM0021620859; the Department of Science and Technology of India; the BK21 and WCU program of the Ministry Education Science and Technology, National Research Foundation of Korea, and NSDC of the Korea Institute of Science and Technology Information; the Polish Ministry of Science and Higher Education; the Ministry of Education and Science of the Russian Federation and the Russian Federal Agency for Atomic Energy; the Slovenian Research Agency; the Swiss National Science Foundation; the National Science Council and the Ministry of Education of Taiwan; and the U.S. Department of Energy. This work is supported by a Grant-in-Aid from MEXT for Science Research in a Priority Area (“New Development of Flavor Physics”), and from JSPS for Creative Scientific Research (“Evolution of Tau-lepton Physics”).

- 
- [1] N. Cabibbo, *Phys. Rev. Lett.* **10**, 531 (1963); M. Kobayashi and T. Maskawa, *Prog. Theor. Phys.* **49**, 652 (1973).  
[2] *CP Violation*, edited by C. Jarlskog, Advanced Series on Directions in High Energy Physics (World Scientific, Singapore, 1989), Vol. 3.  
[3] I. Duniety and R. G. Sachs, *Phys. Rev. D* **37**, 3186 (1988); I. Duniety, *Phys. Lett. B* **427**, 179 (1998); D. A. Suprun,

C. W. Chiang, and J. L. Rosner, *Phys. Rev. D* **65**, 054025 (2002).

- [4] F. J. Ronga *et al.* (Belle Collaboration), *Phys. Rev. D* **73**, 092003 (2006); B. Aubert *et al.* (BABAR Collaboration), *Phys. Rev. D* **73**, 111101 (2006).  
[5] K. F. Chen (Belle Collaboration), *Phys. Rev. Lett.* **98**, 031802 (2007).

- [6] B. Aubert (*BABAR* Collaboration), *Phys. Rev. D* **79**, 072009 (2009).
- [7] D. Choudhury, D. Indumati, A. Soni, and S. Uma Sankar, *Phys. Rev. D* **45**, 217 (1992); C. S. Kim, Y. Kwon, J. Lee, and W. Nangung, *Phys. Rev. D* **63**, 094506 (2001); C. S. Kim and Y. Li, arXiv:1007.2291v2.
- [8] B. Blok, M. Gronau, and J.L. Rosner, *Phys. Rev. Lett.* **78**, 3999 (1997); D. Du, L. Guo, and D. Zhang, *Phys. Lett. B* **406**, 110 (1997); C. K. Chua, W. S. Hou, and K. C. Yang, *Phys. Rev. D* **65**, 096007 (2002); C. W. Chiang, Z. Luo, and J.L. Rosner, *Phys. Rev. D* **66**, 057503 (2002); N. Mahajan, *Phys. Lett. B* **634**, 240 (2006).
- [9] C.D. Lu and K. Ukai, *Eur. Phys. J. C* **28**, 305 (2003); M. Gronau and J.L. Rosner, *Phys. Lett. B* **666**, 185 (2008).
- [10] P. Krokovny *et al.* (Belle Collaboration), *Phys. Rev. Lett.* **89**, 231804 (2002).
- [11] B. Aubert *et al.* (*BABAR* Collaboration), *Phys. Rev. D* **78**, 032005 (2008).
- [12] S. Kurokawa and E. Kikutani, *Nucl. Instrum. Methods Phys. Res., Sect. A* **499**, 1 (2003), and other papers included in this volume.
- [13] A. Abashian *et al.* (Belle Collaboration), *Nucl. Instrum. Methods Phys. Res., Sect. A* **479**, 117 (2002).
- [14] Unless explicitly stated otherwise, inclusion of charge conjugate processes is implied throughout the paper.
- [15] K. Nakamura *et al.* (Particle Data Group), *J. Phys. G* **37**, 075021 (2010).
- [16] K.F. Chen *et al.* (Belle Collaboration), *Phys. Rev. D* **72**, 012004 (2005).
- [17] G.C. Fox and S. Wolfram, *Phys. Rev. Lett.* **41**, 1581 (1978); The modified moments used in this paper are described in S.H. Lee *et al.* (Belle Collaboration), *Phys. Rev. Lett.* **91**, 261801 (2003).
- [18] For MC event generation, the EVTGEN package, described in D.J. Lange, *Nucl. Instrum. Methods Phys. Res., Sect. A* **462**, 152 (2001), is used, while the detector response is simulated using GEANT3, described in R. Brun *et al.*, CERN Report No. CERN-DD-EE-84-1, 1987.
- [19] E. Follana *et al.* (HPQCD and UKQCD Collaborations), *Phys. Rev. Lett.* **100**, 062002 (2008).
- [20] M. A. Baak, Ph.D. thesis, Vrije University [SLAC Report No. SLAC-R-858, 2007].
- [21] N.J. Joshi *et al.* (Belle Collaboration), *Phys. Rev. D* **81**, 031101 (2010).